ingegneria sismica
International Journal of Earthquake Engineering
Anno XLIII - Num. 1 - 2026

Timeliness Optimization Problem and Adaptive Neural Network Application in Fresh Food Logistics Supply Chain Collaboration

Xingmin Qi[1], *Mingcheng Wang*[2,*] *and Xiaowei Xiang*[3]

[1] Productivity Promotion Center, Hubei Institute of Logistics Technology, Xiangyang, Hubei, 441100, China
[2] School of Marxism, Nanning Institute of Technology, Nanning, Guangxi, 530006, China
[3] Scientific Research Department, Hubei Institute of Logistics Technology, Xiangyang, Hubei, 441100, China

SUMMARY: *The current study puts forward the idea of decision-making based on collaboration between the demand forecasting and logistics coordination process of fresh food, using improved PSO-BP neural network. The BP neural network is reinforced through application of PSO technology that incorporates optimized inertia weight, environmental awareness, and solution jumping technique, thus enhancing the accuracy of fresh food demand prediction. Also, the study formulates the multi-constraint and multi-objective optimization model with consideration of time and cost-related factors. The proposed model is then solved using simulated degradation ant colony algorithm, thereby widening the space for finding the optimal solution. The empirical analysis results reveal that the IPSO-BP model demonstrates better performances in comparison with ordinary BP and PSO-BP models in terms of various criteria. For instance, applying the multi-objective distribution model in City A leads to emergence of five optimization routes and decreases the logistics costs, complying with timeliness and load capacity requirements. Thus, the study makes important theoretical and practical contributions to the development of intelligent collaborative optimization of fresh food logistics supply chain.*

KEYWORDS: *IPSO-BP neural network; multi-objective optimization model; ant colony algorithm; fresh food logistics supply chain; timeliness optimization*

1 Introduction

In recent years, the vigorous development of e-commerce platforms has ensured that the demands of logistics services of fresh foods remain increasing steadily, as the circulation of fresh food is now performed via both online and offline operations. Because perishable goods like fruit, vegetables, meats, and seafood are prone to loss during their circulation process, as a result of their physical state along with biological properties, such as high moisture content and respiration, which make them more vulnerable during warehouse processes and transportation, plus possible physical damage during transportation, it is imperative that timeliness be emphasized in fresh food logistics [1-5]. Fast transportation from origin to consumers is desirable, but on another note, it must be ensured that the freshness and quality of perishable goods be maintained at all stages of acquisition, collection, packaging, warehouse storage, transportation, and consumption. Efficient flow of information and coordination at each stage

*wmc_02401@163.com
https://doi.org/10.65102/is2026182
Published: 30 April, 2026

can effectively help improve delivery timeliness, but unfortunately, there are a lot of cases where information asymmetry exists among the different nodes in current supply chains, thus reducing the efficiency of coordination significantly [6-8]. The cold chain logistics does not always work properly as a chain because of insufficient temperature and humidity control when transferring them, thereby worsening their quality and accelerating spoilage [9, 10]. As fresh food is highly sensitive to climate and transportation conditions, these problems become worse in cross-regional transportation [11]. Timeliness of logistics cooperation will reduce benefits and competitive advantage of providers and logistics businesses, and at the same time decrease customers' satisfaction, causing excessive waste [12]. Therefore, improving collaborative timeliness has become a key issue in fresh-produce supply-chain management.

Literature [13] describes a procurement auction model that includes timeliness and sustainability, using the concept of fourth-party logistics and collaborative transportation allocation of third-party logistics considering demand uncertainty under the combination of the enhanced double decomposition algorithm and Lagrangian relaxation. The proposed method increases coordination efficiency and transportation timeliness in fresh agricultural product transport. Literature [14] focuses on minimizing cargo loss and lowering distribution costs, improving customer satisfaction through constructing a cold-chain optimization model using a multi-objective function and genetic algorithm. It demonstrates that the proposed method is effective in balancing loss and efficiency. Literature [15] establishes a model for optimizing vehicle paths in cold-chain logistics, aiming at minimizing delivery cost and food safety risk, which uses an adaptive improved ant colony algorithm for congestion control, cold storage temperature control, minimizing total cost, and protecting food quality. Literature [16] develops an intelligent optimization method by utilizing an adaptive elite-preserving genetic algorithm and a multilayer perceptron to deal with information island problems in cold chain logistics. The results show a reduction in temperature abnormality rate, distribution time, and transportation cost by 70%, 20.7%, and 15.2%, respectively, as well as increasing operational efficiency and supply chain reliability. However, adaptive approaches still demonstrate inadequate environmental adaptability and weak generalization ability.

And literature [17] artificial neural networks are used to optimize food logistics management, leading to operational effectiveness and customer satisfaction due to efficient coordination of supply and demand. Besides, such a model can reduce costs of labor and resources, as well as enable process optimization. An adaptive neural network, which changes its parameters and network architecture by means of adaptive learning algorithms, is especially useful for revealing the peculiarities of input data. Literature [18], principal component analysis and a backpropagation neural network are employed for improving forecast accuracy in cold chain logistics. Literature [19] applies a Bayesian optimized bidirectional long short-term memory network to inventory demand forecast in cross-border cold chain logistics, serving as a good technical solution that minimizes logistics and warehouse waste. Literature [20] , a deep convolutional neural network is applied to estimate the shelf life of fruits and vegetables by considering transportation and storage temperature, thus contributing to logistics decision-making and waste prevention. Literature [21] designs a perishable inventory control system under uncertain deterioration conditions using BPNN and robust multi-criteria optimization; spoilage is modeled using the Weibull distribution, making it possible to find a good trade-off between inventory quantity and waste. Literature [22] designs a perishable inventory control system under uncertain deterioration conditions using BPNN and robust multi-criteria optimization; spoilage is modeled using the Weibull distribution, making it possible to find a good trade-off between inventory quantity and waste. Literature [23] developed a neural network model based on LSTM and deep neural network, etc., combined with multi-source data,

which can realize real-time accurate estimation of food temperature in cold chain logistics supply chain in multi-temperature zone transportation vehicles, and significantly improve the accuracy and reliability of monitoring. Literature [24] integrates 5G, distributed sensors and LSTM prediction to establish an intelligent network system, which realizes accurate and efficient regulation of heat and temperature in agricultural storage logistics through high-throughput humidification technology and reinforcement learning algorithms, and improves energy efficiency and control response speed.

The present research work provides a new framework based on artificial neural networks for forecasting the demand in fresh produce logistics, and makes improvements in the classical PSO algorithm by optimizing the inertia weights, designing an environmental detection scheme, and introducing a jump-out solution technique. The BP neural network is further trained using the modified PSO, and thus enables the forecast of demand in fresh produce through the IPSO-BP model. An optimization model consisting of multi-objective functions in terms of transportation distance cost, carbon emission cost, damage cargo cost, and fixed cost of vehicles is proposed. The optimization problem is solved using the ACO algorithm. In order to solve the problem of premature convergence and low global search ability in the traditional ACO, a simulated annealing technique is introduced to improve climbing ability.

2 Fresh food supply demand forecasting model based on IPSO - BP

2.1 Demand forecasting model for fresh supply

The core of the fresh-supply strategy in collaborative manufacturing service value chains can be understood as a forward-looking coordination process that allocates resources to improve the delivery of goods and services, facilitate information exchange, and balance supply with demand between manufacturers and customers. Figure 1 illustrates a three-tier fresh-food supply-chain network, in which the flows of products and information are represented by solid and dashed lines, respectively.

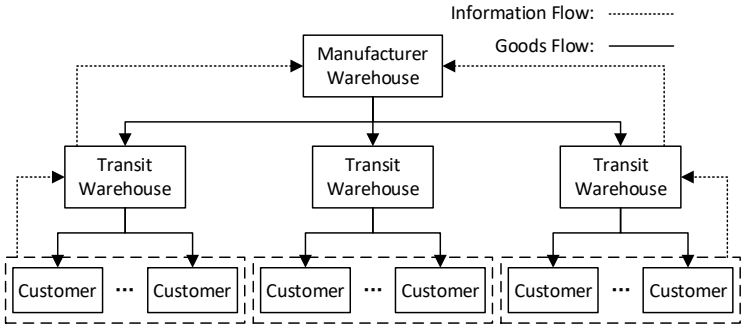

Figure 1: Three-level supply chain network for spare parts

In fact, different customer vendors will have different lead times depending on the demand situation, therefore, under the (T, S_t) inventory strategy, the time interval T is used as a fixed checking cycle to dynamically query the customer's inventory data, and combined with the fresh supply model in this paper, by accurately calculating the ordering points and order quantities of different customer vendors, it can be ensured that the inventory cost can be reduced at the while reducing the number of stock-outs.

The model is based on the following assumptions:

(1) Manufacturer's production capacity and transit warehouse stock capacity are infinite, so the problem of oversupply in manufacturer's production and the problem of transit warehouse stock cost are not considered.

(2) The per-unit transportation cost and travel time from the manufacturer’ s warehouse to the transit warehouse, as well as those from the transit warehouse to the customer, are assumed to be known constants. In addition, the distances between each customer manufacturer and every transit warehouse are taken to be identical.

(3) Lead time refers to the transportation period within the fresh-supply process. Each customer vendor is assumed to have the same level of importance, its maximum inventory capacity is predetermined, and the inventory review cycle is set to be equal to the lead time of the fresh supply.

The model aims to estimate the quantity of spare parts required at time t when the inventory review node reaches t, and then optimize the system through an improved particle-swarm-based BP neural network so as to minimize the overall cost. The total cost is composed of inventory cost, shortage cost, ordering cost, and transportation cost. The objective function adopted in this study is given in Equation (1).

$$\begin{aligned}\min Z_j^t = C_j^t \times \left(O_j^t - \left(T_j^t \times D_j^t\right)\right) \times \alpha(t) + S_j^t \times \left(\left(T_j^t \times D_j^t\right) - O_j^t\right) \\ \times \alpha(t) + \left(P_j^t \times Q_j^t + L_{ij}^t \times Q_j^t\right) \times \beta(t)\end{aligned} \tag{1}$$

where $\alpha(t)$ is the formula for determining whether customer vendor j is out of stock at moment t, as shown in equation (2).

$$\alpha(t) = \begin{cases} 1, \left(T_j^t \times D_j^t\right) > O_j^t \\ 0, \left(T_j^t \times D_j^t\right) \le O_j^t \end{cases} \tag{2}$$

$\beta(t)$ is the determination formula for whether customer vendor j needs to make an order at moment t, i.e., the determination formula for whether customer vendor j defines moment t as an ordering point is shown in equation (3).

$$\beta(t) = \begin{cases} 1, \dfrac{O_j^t - \left(T_j^t \times D_j^t\right)}{D_j^t} \le T_j^t \\ 0, \dfrac{O_j^t - \left(T_j^t \times D_j^t\right)}{D_j^t} > T_j^t \end{cases} \tag{3}$$

Then the total target cost of all customer vendors at moment t is shown in equation (4).

$$Z^t = \sum_{j=1}^{J} Z_j^t \tag{4}$$

The constraints of the above equation are shown in equation (5).

$$\begin{cases} \left| O_j^t - \left(T_j^t \times D_j^t \right) \right| + Q_j^t \le V_j \\ \sum_{j=1}^{J} Q_j^t \le W_i \end{cases} \tag{5}$$

In this study, a BP neural network optimized by an enhanced particle swarm algorithm is used to forecast spare-parts demand at the order point t, and the corresponding ideal expected output for the optimal prediction is expressed in Equation (6).

$$Q_{j,BEST}^t = D_j^t \times 2T_j^t - O_j^t \tag{6}$$

2.2 Improvement of Particle Swarm Optimization Algorithm

The weight factor controls the trade-off between global and local searching abilities of the proposed algorithm. The greater inertia weight causes better velocities in the starting trajectory, leading to the exploration of remote areas and hence providing better global searching ability in standard PSO. On the other hand, the lower inertia weight reduces the velocities of the particles, resulting in better local searching abilities. Generally speaking, a strong searching ability is desirable in the beginning, but an intensified local search is preferred as the iteration progresses. Thus, a comparatively higher value for the weight factor is set in the early part of the algorithm execution in order to allow the exploration of the search space, while a comparatively lower one will be chosen after that to emphasize local searching. Hence, the inertia weight must first be allowed to diminish in a non-linear manner before being made to decrease linearly.

The function to construct the inertia weights is shown in equation (7).

$$\omega(k) = \begin{cases} \omega_{\min} + \left(\omega_{\max} - \omega_{\min} \right) \times s_1(k), & k < L \\ \omega_{\max} - \left(\omega_c - \omega_{\min} \right) \times s_2(k), & k \ge L \end{cases} \tag{7}$$

The derivation of $s_1(k)$ and $s_2(k)$ values is shown in the following equation.

$$s_1(k) = \frac{1}{1 + e^{-(k/K)}} \tag{8}$$

$$s_2(k) = -\frac{2k}{K} \tag{9}$$

where k is the current number of iterations, K is the maximum value of the number of iterations, $\omega_{\max}$ and $\omega_{\min}$ denote the maximum and minimum values of the inertia weights, respectively, $s_1(k)$ is a nonlinear function, $s_2(k)$ is a linear function, and ω_c is the initial value of the inertia weight after the particle undergoes a search .

During the course of optimizing using particle swarm optimization, change in the model parameters could affect the entire environment for the optimization process. In order for this to be achieved, it is imperative that the particle swarm optimization algorithm recognize the change and respond accordingly. To ensure this, an environment detector was introduced.

The environment detector algorithm is shown in equation (10).

$$\begin{aligned} Detector_t = &\operatorname{sgn}\left(\left|\exp\left(\lambda_1^t - \lambda_1^{t-1}\right) - 1\right|\right) \cup \operatorname{sgn}\left(\left|\exp\left(\lambda_2^t - \lambda_2^{t-1}\right) - 1\right|\right) \\ &\cup \cdots \cup \operatorname{sgn}\left(\left|\exp\left(\lambda_n^t - \lambda_n^{t-1}\right) - 1\right|\right) \end{aligned} \tag{10}$$

Once a change has been identified, it will be important to reconsider the problem optimization by incorporating the new environment. A simple method could involve resetting the particles; but then, the convergence rate could decrease. On the other hand, keeping particle positions could, due to memory of the algorithm, lead to stagnation within a local optima. For this reason, there is a need to modify the particle positions without compromising on the convergence rate; hence, an adaptive jumping scheme comes in handy.

When there is environmental variability during iterations, the basic particle swarm optimization becomes prone to convergence into local optima due to the inability of the particles to explore further. To solve this problem and inspired by the concept of mutation within genetic algorithms, a mutation particle will be employed as part of the jumping solution scheme. Whenever there is change in the environment, this mutation particle will ensure transition of particles into different areas. With this strategy, there is no chance that particles become trapped within local optima and the ability to find a global optimum is enhanced. The mathematical expression for this scheme is given in equation (11).

$$x_i^t = x_i^t + s \tag{11}$$

where t is the iteration depth when falling into the local optimum solution, s is the regulated search length, and the function expression is shown in equation (12).

$$s = \frac{u}{|v|^{\frac{1}{\beta}}} \tag{12}$$

where $u \sim N(0, \sigma_u^2)$ and $v \sim N(0,1)$, both of which have mean values equal to 0, and the variance expression is shown in equation (13).

$$\sigma_u = \left\{ \frac{\Gamma(1+\beta)\sin\left(\frac{\beta\pi}{2}\right)}{\Gamma\left(\frac{1+\beta}{2}\right)\beta^{2^{\left(\frac{\beta-1}{2}\right)}}} \right\}^{\frac{1}{\beta}}, \sigma_v = 1 \tag{13}$$

where $\Gamma(x) = \int_0^\infty t^{x-1}e^{-t}dt$, the particle alternates between small and large distance updates during the position update process, which is more helpful for the particle to jump out of the local optimal solution and expand the overall search area.

2.3 Improved particle swarm algorithm to optimize BP neural network

Because BP neural networks are highly sensitive to parameter settings such as connection weights and thresholds, these factors have a direct influence on prediction accuracy. Therefore, the BP neural network parameters are optimized by the improved particle swarm algorithm. The corresponding optimization flow is presented in Figure 2.

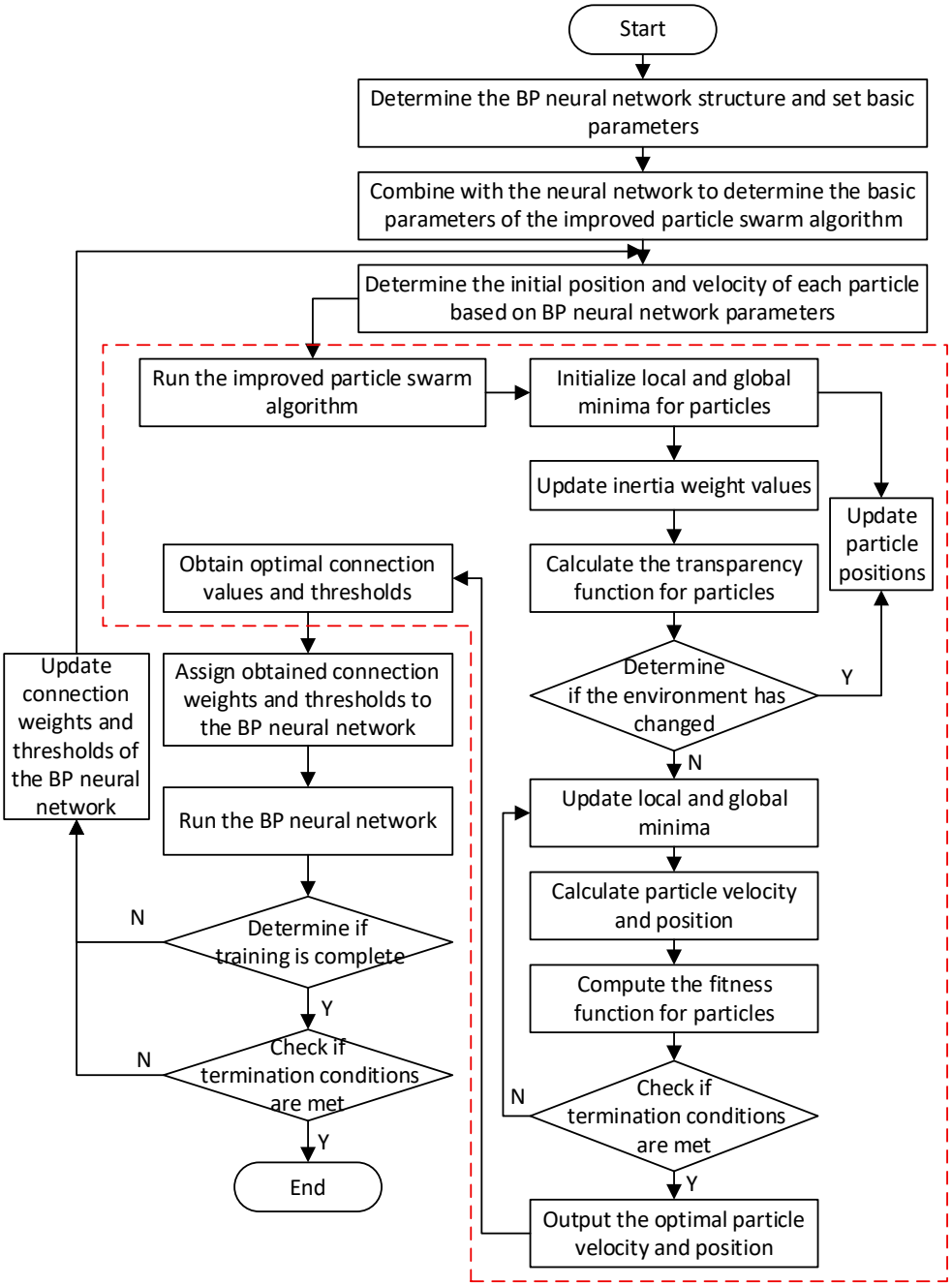

Figure 2: IPSO algorithm optimizes BP neural network flow chart

3 Fresh food logistics supply chain distribution path optimization model considering timeliness

3.1 Problem description and model construction

In this research work, a routing and distribution problem is analyzed where vehicle speeds are not constant but change according to time; the main aim of such a problem is to optimize the time-sensitive process in the context of logistics supply chain for fresh food products. The mathematical formulation of this problem can be stated as follows: A logistics distribution center deploys various vehicle types to transport commodities to the customers located in

diverse urban areas; demand and location information of customers are provided, time window considerations apply, and time-varying vehicle speeds arise due to environmental circumstances. The objective of optimization here includes determining the dispatching and routing policy.

To support the analysis and solution of this problem, the following assumptions are adopted:

(1) The coordinates of the distribution center and customer nodes are known, and all vehicles depart from and return to the distribution center.

(2) The depot contains several categories of delivery vehicles, but the number available in each category is limited.

(3) Travel speed varies across different time periods.

(4) Each customer is assigned a fixed delivery time window, and penalties are imposed for early arrival or late service.

(5) Each customer is served by only one vehicle, and the required demand must not exceed the maximum load capacity of that vehicle.

(6) Different vehicle categories have different maximum capacities, fixed operating costs, fuel-consumption rates, and carbon-emission coefficients.

(7) No fuel is consumed and no carbon emissions are produced during vehicle waiting or service time.

3.2 Modeling

There are several parameters that have an effect on the speed of delivery vehicles. Traditional modeling studies in relation to vehicle routing are based on stationary speed. In real-life scenarios, speed varies over time and should be assumed to be time-dependent. This study focuses on the impact of the two periods of congestion on the vehicle speed under sunny weather condition.

Based on previous studies and observations, we develop a time-dependent speed model in relation to sunny weather for different periods of congestion. The influence coefficient of a particular period on the speed of the vehicle during sunny weather is formulated as ζ_{sun}:

$$\zeta_{sun}=\begin{cases}0 & 0\le t<6 \ Or \ 22\le t<24\\ 0.225t-1.35 & 6\le t<8\\ -0.05t+0.85 & 8\le t<12\\ \dfrac{t}{30}-0.15 & 12\le t<18\\ -0.1125t+2.475 & 18\le t<22\end{cases} \tag{14}$$

where t is the point in time where the vehicle is traveling.

The vehicle speed $\hat{S}_v$ under different time periods is calculated as in Equation (15) for sunny days:

$$\hat{S}_v=\bar{S}_v\cdot\left(1-\zeta_{sun}\right) \tag{15}$$

where $\bar{S}_v$ is the average traveling speed of the distribution vehicle, km/h.

Therefore, the traveling time of the distribution vehicle in traveling from any point i to j is denoted as:

$$t_{ij} = \frac{d_{ij}}{\hat{S}_v} \tag{16}$$

where t_{ij} is the time taken by the distribution vehicle from point i to point j, h; d_{ij} is the distance from any customer point i to j, km.

The calculation of fuel consumption and carbon emission of different types of vehicles will be affected by many factors, among which the load weight is the most important one.

Then we calculate the CO_2 emission factor of each type of truck according to the principle of carbon balance, and finally take the average value of the results of each truck as the carbon emission factor of the vehicle.

Therefore, the carbon emission cost C_2 of different models of operating vehicles is calculated as shown in Equation (17).

$$C_2 = \sum_{m=1}^{M} \sum_{i=0}^{n} \sum_{j=0}^{n} x_{ijk}^{m} \cdot E^{m} \cdot L_{ij} \tag{17}$$

where x_{ijk}^{m} is a 0 to 1 variable; $x_{ijk}^{m} = 1$ if the model is m vehicle k from point i to point j; otherwise $x_{ijk}^{m} = 0$. E^{m} is the carbon emission factor of model m, g/km. L_{ij} is the distance from any customer point i to j, km.

In this study, cargo-loss cost is divided into two parts: in-transit loss and unloading loss.

(1) In-transit cargo damage cost. This refers to the loss that results from the effects of temperature, moisture, and other conditions experienced during transportation to the destination customer node by the truck. Due to their highly perishable nature, the loss resulting from transportation is expected to be directly proportional to the length of time for which the transportation process takes place.

$$\theta_1 = \left(1 - e^{-\varepsilon\left(T_i^A - T_{i-1}^L\right)}\right) \tag{18}$$

where ε is the product spoilage rate, %, the larger the value, the more serious the spoilage of the product per unit of time; T_i^A is the earliest point of time for the service to start at customer point i, h; and T_{i-1}^L is the latest point of time for the service at the previous point of customer point i, h.

The cost of in-transit cargo damage C_3^1 is calculated as:

$$C_3^1 = \sum_{m=1}^{M} \sum_{i=0}^{n} x_i^m \, pQ_i\theta_1 \tag{19}$$

where x_i^m is a 0 to 1 variable: $x_i^m = 1$ if customer point i is served by a vehicle of model m; otherwise $x_i^m = 0$. p is the unit price of fresh goods, yuan. Q_i is the load of the distribution vehicle when it arrives at point i, %.

(2) Unloading cargo damage cost. This term arises when the delivery vehicle reaches the customer node and the compartment door is opened for unloading, leading to product loss and related expenses. Assuming that the unloading loss coefficient per unit time and cargo weight

is:

$$\theta_2 = \left(1 - e^{-\varepsilon T_{si}}\right) \tag{20}$$

where T_{si} is the service time, h, at customer point i.

The cost of cargo damage at unloading C_3^2 is Equation (21), and the total cargo damage cost C_3 is calculated as Equation (22):

$$C_3^2 = \sum_{m=1}^{M}\sum_{i=0}^{n} x_i^m p\theta_2 \left(Q_i - q_i\right) \tag{21}$$

$$C_3 = C_3^1 + C_3^2 \tag{22}$$

where q_i is the demand of goods at customer point i, kg.

The fixed operating cost of a vehicle mainly consists of vehicle-use cost, labor cost during driving and unloading, and the fixed activation cost of the delivery vehicle. The vehicle fixed cost C_4 is expressed as follows:

$$\begin{aligned} C_4 = &\sum_{m=1}^{M}\sum_{k=1}^{K}\sum_{i=0}^{n}\sum_{j=0}^{n} x_{ijk}^m \cdot t_{ij} \cdot \left(\mu_k + P_m\right) \\ &+ \sum_{m=1}^{M}\sum_{k=1}^{K}\sum_{i=0}^{n} Y_{ik}^m \cdot s_i \cdot \left(\mu_k + P_m\right) + \sum_{m=1}^{M}\sum_{k=1}^{K}\sum_{i=0}^{n} X_{0jk}^m \cdot \zeta_m \end{aligned} \tag{23}$$

where μ_k is the cost per unit time of using vehicle k, yuan; P_m is the cost per unit time of labor for using vehicle of type m, yuan; ζ_m is the cost of a fixed dispatch of vehicle of model m, yuan; and X_{0jk}^m is a variable of 0~1: if vehicle k of model m travels from the distribution center to point j, then $X_{0jk}^m = 1$, otherwise $X_{0jk}^m = 0$; Y_{ik}^m is a 0~1 variable: if vehicle k of model m passes through point i, then $Y_{ik}^m = 1$, otherwise $Y_{ik}^m = 0$.

3.3 Multi-objective optimization modeling of distribution paths

Under the consideration of driving speed, vehicle carbon emission and cargo damage cost, time window, and multiple vehicle models to meet the needs of all customers, and with the objective of the lowest driving distance C_1, carbon emission cost C_2, cargo damage cost C_3, and vehicle fixed cost C_4, and the comprehensive consideration of the above four objective functions, the multi-objective joint optimization model for the optimization of the delivery path of the fresh food e-commerce company is shown below:

$$\min C_1 = \sum_{i=0}^{n}\sum_{j=0}^{n}\sum_{k=1}^{M} d_{ij} x_{kij} \tag{24}$$

$$\min C_2 = \sum_{m=1}^{M}\sum_{i=0}^{n}\sum_{j=0}^{n} x_{ij}^m \cdot E^k \cdot L_{ij} \tag{25}$$

$$\begin{aligned}\min C_3 = C_3^1 + C_3^2 = &\sum_{m=1}^{M}\sum_{i=0}^{n} x_i^m \, pQ_i\theta_1\left(T_i^A - T_{i-1}^L\right) \\ &+\sum_{m=1}^{M}\sum_{i=0}^{n} x_i^m \, p\theta_2\left(Q_i - q_i\right)T_{si}\end{aligned} \tag{26}$$

$$\begin{aligned}\min C_4 = &\sum_{m=1}^{M}\sum_{k=1}^{K}\sum_{i=0}^{n}\sum_{j=0}^{n} x_{ijk}^m \cdot t_{ij} \cdot \left(\mu_k + P_m\right) \\ &+\sum_{m=1}^{M}\sum_{k=1}^{K}\sum_{i=0}^{n} Y_{ik}^m \cdot s_i \cdot \left(\mu_k + P_m\right) + \sum_{m=1}^{M}\sum_{k=1}^{K}\sum_{i=0}^{n} X_{0jk}^m \cdot \zeta_m\end{aligned} \tag{27}$$

where x_{kij} is a 0 to 1 variable: if vehicle k goes from point i to point j, then $x_{kij}=1$, otherwise $x_{kij}=0$.

3.4 Distribution path multi-objective optimization model solution

3.4.1 Ant colony algorithm solution

Consider that there are m vehicles (ants) positioned on n demand points. In every step, each of the vehicles selects the next unvisited demand point based on certain conditions, and after the move from one point to another, or when one cycle of visiting n demand points is completed, the pheromone amount on the paths is recalculated.

Suppose that there are n demand points in total and m vehicles (number of ants):

$$\mathrm{m} = \sum_{i=1}^{n} b_i(t) \tag{28}$$

The number of vehicles (ants) located at demand point i at time t and satisfying $\Gamma = \{\tau_{ij(t)}\}$.

The Γ denotes the set of pheromone concentrations on the distribution path at moment t. $\tau_{ij(t)}$ denotes the pheromone concentration on the path (i, j) at moment t.

$$P_{ij(t)}^k = \begin{cases} \dfrac{\left[\tau_{ij(t)}\right]^{\alpha}\left[\eta_{ij(t)}\right]^{\beta}}{\sum_{s\in allowed_k}\left[\tau_{is(t)}\right]^{\alpha}\left[\eta_{is(t)}\right]^{\beta}} & j \in allowed_k \\ 0 & else \end{cases} \tag{29}$$

α is the information heuristic factor, indicating the relative importance of paths;

β is the expectation heuristic factor, indicating the relative importance of visibility;

$allowed_k = \{\cdots 0, 1, n-1\}$, which represents all nodes that vehicle k can currently select;

$tabu_k$ is a taboo table used to record the nodes that the vehicle (ant) has currently traveled through;

$\eta_{ij}(t)$ is the visibility at moment t, which indicates the degree of predictability for the vehicle (ant) to move from node i to node j.

Using the tabu list, data for each customer who has already been served is entered and kept

up-to-date during the search process. Once the specified number of steps have been achieved, the search process stops. At this point, all tabu lists will be full, and the distances traveled by each ant can be determined, which will be used to get the optimal solution. After obtaining the optimal solution, the pheromones in the optimal path will be updated based on the equation.

After reaching the predetermined upper bound, the final result will be the shortest distance that can be achieved by the vehicle. The pheromone updating scheme is shown below:

$$\tau_{ij}(t+n) = \rho \cdot \tau_{ij}(t) + \Delta\tau_{ij} \tag{30}$$

$$\Delta\tau_{ij}(t+n) = \sum_{k=1}^{m} \Delta\tau_{ij}^{k} \tag{31}$$

3.4.2 Simulated Annealing Ant Colony Algorithm

The implementation of ant colony optimization (ACO) algorithm requires extensive computations, as well as sensitivity to falling into a non-viable area in complicated settings. Detouring in routes might also cause the algorithm to take longer to produce solutions. In reality, the algorithm might take longer to converge on a solution due to inadequate starting pheromones in an optimization scenario. However, since the aim of the algorithm is to find an optimal solution for all the ants, the computation time could also be compromised in the process. Lastly, because of its quick convergence nature, the ACO algorithm cannot discover the global optimum point while computing.

Simulated annealing is inspired by the concept of annealing, which is seen in solid-state physics and refers to a process that involves probability-based optimization. In this process, a solid substance is initially heated to temperatures that are relatively high and then cooled at a gradual pace. When there is heating in this process, an increase in temperature leads to disorganization in the arrangement of the particles inside the system, causing increased internal energy levels in the system. As a result of gradual cooling, particles organize into an orderly structure at each level of temperature.

In this study, simulated annealing is incorporated into the ACO framework to enhance the search mechanism. After the ant colony search is completed, the annealing procedure is further used to strengthen neighborhood exploration and improve the climbing capability of the algorithm, thereby compensating for the limited global-search performance of the original ant colony method.

Simulated annealing consists of two components: the Metropolis criterion and the annealing process.

Annealing process: jumping out of the local optimum is the core of annealing.

Metropolis algorithm: let the previous state be $X(n)$ and the system energy be $E(n)$, according to the system metrics (energy from the previous section, gradient descent), the state changes to $X(n+1)$, and, at the same time, the system energy becomes $E(n+1)$, which defines the probability of acceptance P for the system to change from $X(n)$ to $X(n+1)$:

$$P = \begin{cases} 1 & E(n+1) < E(n) \\ e^{-\frac{E(n+1)-E(n)}{T}} & E(n+1) \geq E(n) \end{cases} \tag{32}$$

When the energy decreases, the probability $P = 1$, that is, this transfer is accepted; when the energy increases, the system deviates more from the global optimum, and the probability is judged: in the interval $[0,1]$ for ϵ a uniformly distributed random number, if $P > \epsilon$, the

transfer can be accepted, otherwise the transfer is rejected, and go to the next step , reciprocal loop.

Parameter control of annealing algorithm: The Metropolis algorithm is the main component of simulated annealing. Nevertheless, the rate of convergence is sometimes inadequate in practical applications. Therefore, the algorithm should be configured properly such that the search time will not exceed some particular limit. The major parameter to be adjusted is T. If T is too large, the cooling process will be too fast and thus the algorithm might converge to a local minimum near the end of the process. On the other hand, T being too small means that the problem would require significant computational effort. For practical applications, a strategy called "cooling schedule" is used: initially, a rather large T value is set, which is then decreased gradually:

(1) The initial temperature $T(0)$ should be chosen high enough so that all transfer states are accepted.

(2) Annealing rate. The most common approach is an exponential decrease.

$$T(n) = \lambda T(n), n = 1, 2, 3, \cdots \tag{33}$$

where λ is a positive number less than 1, typically taking the value $[0.8, 0.99]$. So that for each temperature, sufficient transfers can be attempted, exponential descent converges relatively more slowly, and other descents are as follows:

$$T(n) = \frac{T(0)}{1+t} \tag{34}$$

$$T(n) = \frac{T(0)}{\log(1+t)} \tag{35}$$

(3) Termination temperature. After numerous iterations, annealing is completed when a new state emerges that reaches the specified value.

3.4.3 Steps of the Optimal Path Solving Algorithm

The detailed procedure of the optimal-path search algorithm is described as follows.

Step 1: Set the initial parameters, including ant colony size, pheromone factor, heuristic factor, pheromone evaporation coefficient, pheromone constant, and the upper limit of iterations.

Step 2: Randomly assign vehicles to different demand nodes. Each vehicle continues visiting subsequent demand nodes until all customer nodes have been traversed.

Step 3: Compute the minimum cost, that is, the objective-function value, record the best route obtained in the current iteration, and update the pheromone level along that route.

Step 4: Apply the simulated annealing method to the current result as the starting point for neighborhood search:

(1) Initialization: initial temperature T (sufficiently large), number of iterations L, etc.

(2) Generate new solution S'.

(3) Calculate the increment $\Delta t' = C(S') - C(S)$, where $C(S)$ is the evaluation function.

(4) If $\Delta t' < 0$ then accept S' as the new current solution, otherwise accept S' as the new current solution with probability $\exp(-\Delta t' / T)$.

(5) If the stopping criterion is satisfied, output the current best result; otherwise, repeat from substep (2).

Step 5: Compare the best solution obtained by simulated annealing with the present best result of the ant colony algorithm, and then update the global best solution.

Step 6: If the iteration count has not yet reached the preset maximum, return to Step 2; otherwise, terminate the procedure.

4 Experimental results and analysis

4.1 IPSO - BP based supply demand forecasting results

4.1.1 Parameter configuration

The IPSO-BP neural network used in this experiment was established based on the previous work and its parameters include: population size, N = 60; individual learning factors, the initial and final values were 2.4 and 0.4; social learning factors, the initial and final values were 1 and 2.24; inertia weights, the upper bound and lower bound were 0.85 and 0.35, respectively. Position range of particles: [−1.2, 1.2]; velocity range of particles: [−0.025, 0.025]. Maximum iterations were 600. With respect to the PSO-BP neural network which made use of randomization when initializing the particle swarm, learning factors were both 2, inertia weight was 0.85, and other parameter values were the same with IPSO-BP algorithm. In the BP neural network model, the training goal error is 1×10^{-4}, learning rate is 0.1.

4.1.2 Sample data selection

Indirect estimation of the demand for logistics services connected to fresh agricultural products in City A was performed using the integration of per-capita consumption of different types of goods and the population of the city. Following previous studies in this field, a list of 15 indicators, named B1-B15, covering five main aspects: agriculture supply, socio-economic situation, cold chain development, humanism development, and scale of logistics demand, was created. They include the following: the rate of fresh agricultural products, index of price of fresh agricultural products, production of fresh agricultural products, social capital formation, gross domestic product of the region, primary industry's contribution to GDP, per capita consumption of fresh agricultural products, overall wholesale volume of fresh agricultural products, number of refrigerated trucks, number of enterprises, cold storage capacity, urban resident's per capita consumption expenditure, urban resident population, tertiary industry employment, and number of highway-operated vehicles.

4.1.3 Data pre-processing

Differences in the magnitude of indicator values, caused by differences in scale, may reduce convergence speed and simulation accuracy. Therefore, before model training, both the input and output variables were normalized. In this study, min-max linear normalization was adopted to linearly transform the original values according to the following formula:

$$\delta = \frac{a - a_{\min}}{a_{\max} - a_{\min}} \times \left(z_{\max} - z_{\min} \right) \tag{36}$$

where: δ is the value after normalization; a is the value before normalization; $a_{\min}$ and $a_{\max}$ are the minimum and maximum values of the original data, respectively; $z_{\min}$ and $z_{\max}$

are the lower and upper bounds of normalization, respectively, and in this paper, the data are normalized to the $[0,1]$ interval, so $z_{\min}=0$ and $z_{\max}=1$.

The gray correlation analysis method was then used to measure the strength of relationship among variables and to enable dimension reduction. Before model fitting, the data set was subjected to gray correlation analysis to determine the key variables that were strongly related, using the formula as shown below:

$$\theta_\eta=\frac{1}{m}\sum_{\zeta=1}^{m}\frac{\min\limits_{\eta}\min\limits_{\zeta}\left|x_0(\zeta)-x_\eta(\zeta)\right|+\rho\times\max\limits_{\eta}\max\limits_{\zeta}\left|x_0(\zeta)-x_\eta(\zeta)\right|}{\left|x_0(\zeta)-x_\eta(\zeta)\right|+\rho\times\max\limits_{\eta}\max\limits_{\zeta}\left|x_0(\zeta)-x_\eta(\zeta)\right|} \tag{37}$$

where: θ_η is the gray correlation of the $\eta(\eta=1,2,\cdots,e)$ subsequence; $\zeta(\zeta=1,2,\cdots,m)$ denotes the sequence dimension; $x_0(\zeta)$ is the parent sequence; $x_\eta(\zeta)$ is a subsequence; ρ is the resolution coefficient, generally ρ is taken as $(0,1)$, the smaller ρ the greater the resolution, $\min\limits_{\eta}\min\limits_{\zeta}\left|x_0(\zeta)-x_\eta(\zeta)\right|$ is the two-level minimum difference; $\max\limits_{\eta}\max\limits_{\zeta}\left|x_0(\zeta)-x_\eta(\zeta)\right|$ is the two-stage maximum difference. Finally, the degree of influence of each factor is ranked according to the correlation of each factor. The greater the correlation, the greater the degree of influence of the factors.

4.1.4 Analysis of the results of supply demand forecasts

The normalized data set is divided into a reference series and several comparison series. The demand for fresh agricultural products in City A acts as a reference series, while other influencing factors act as comparison series for the gray relational analysis. The respective statistical data are shown in Table 1.

By applying the method of gray relational analysis, it can be concluded that all fifteen influencing factors discovered in this research have high degrees of relevance to the demand for logistics services of fresh agricultural products in City A, with all correlation coefficients being greater than 0.6, an acceptable value. Among these influencing factors, per capita consumption of fresh agricultural products, the commodity index of fresh agricultural products, cold storage capacity, the population of city residents, and the total wholesale sales of fresh agricultural products are highly correlated with a correlation degree of more than 0.6. Accordingly, five factors with higher correlation coefficients (more than 0.85) are selected as major influencing factors.

Table 1: Analysis of grey correlation analysis

Evaluation item	Correlation degree	Ranking
Consumption of raw produce per capita	0.951	1
The commodity rate of fresh agricultural products	0.875	2
Cold storage capacity	0.866	3
Urban permanent population	0.856	4
Wholesale production of fresh agricultural products	0.852	5
Production price index for raw produce	0.806	6
Annual production of raw produce	0.790	7
Enterprise quantity	0.769	8
Urban residents per capita consumption expenditure	0.726	9
Car ownership of highway	0.718	10
Social fixed asset investment	0.697	11
Tertiary industry personnel	0.693	12
The added value of the first production	0.664	13
Regional GDP	0.639	14
The number of refrigerated vehicles	0.617	15

For the analysis, the selected indicators included per capita consumption of fresh agricultural products, commodity rate of fresh agricultural products, cold storage capacity, number of urban residents, and the total volume of fresh agricultural products at wholesale markets. In the case of logistics demand for fresh agricultural products in City A, it is taken as the target output variable. All these data were analyzed using BP, PSO-BP, and IPSO-BP neural network models. Apart from considering the fitting degree between predictions and real values, three kinds of error metrics including MAPE, MAE, and RMSE were used to conduct model evaluation. The forecasted results of these models are demonstrated in Figure 3, where there exist apparent differences among the three models. In particular, the IPSO-BP neural network model performs better than others, and it shows that the prediction results approach the real values. As shown in Table 2, the MAPE, MAE, and RMSE results of three models were compared with each other. It is obvious that all the results in IPSO-BP model are smaller than those in BP and PSO-BP models, with an MAPE of 0.15%.

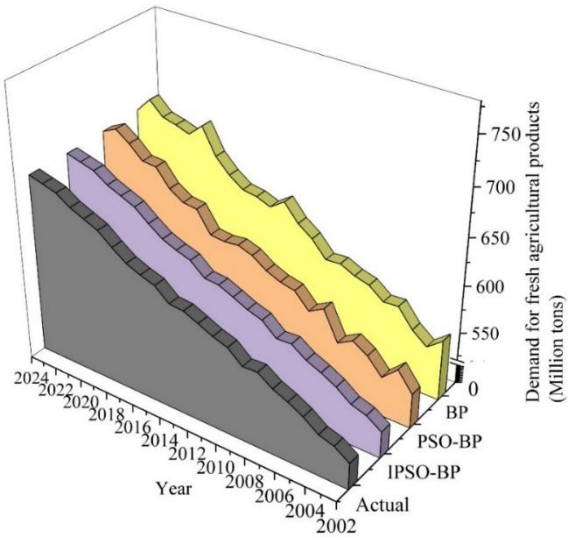

Figure 3: Prediction of different models

Table 2: The prediction error of three neural network models is compared

Model	MAPE/%	MAE/Million tons	RMSE/Million tons
BP	2.58	13.546	15.306
PSO-BP	0.92	5.456	6.725
IPSO-BP	0.15	1.023	1.564

Convergence performance of the three NN models is shown in Figure 4. In this case, the IPSO-BP NN shows higher convergence performance and better prediction accuracy when compared to PSO-BP and BP NNs. The optimum performance of the IPSO-BP NN is achieved after approximately 210 iterations while that of the PSO-BP and BP NNs is achieved after about 350 and 460 iterations, respectively. Therefore, the IPSO-BP NN model performs better than the PSO-BP and BP NNs in terms of prediction accuracy and convergence performance and is feasible for predicting logistics demands of fresh agricultural produce.

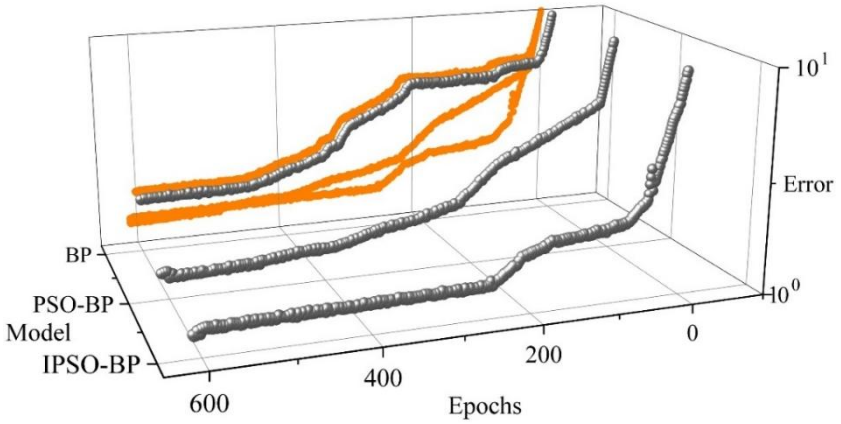

Figure 4: The evolution of three neural networks

Finally, the IPSO-BP neural network model was applied to predict the demand for logistics of fresh agricultural produce in City A. In the beginning, the gray predictive technique that was available in the SPSS software tool box was used to predict the significant factors, whose predictions are indicated in Table 3 from 2025 to 2029. After that, these predicted factors were entered into the model for predicting the logistics demand for fresh agricultural produce in City A. The predicted demands for the years 2025, 2026, 2027, 2028, and 2029 are 6,550,500 tons, 6,763,700 tons, 6,712,500 tons, 6,791,600 tons.

Table 3: Predictions for 2025 to 2029

Year	Consumption of raw produce per capita/kg	The commodity rate of fresh agricultural products/%	Cold storage capacity/t	Urban permanent population/ 10,000	Wholesale production of fresh agricultural products/Hundred dollars
2025	254.251	86.341	4640845	2576.405	3950.321
2026	259.916	86.556	4942895	2602.265	4166.215
2027	255.692	86.768	5253188	2625.231	4388.215
2028	256.451	86.965	5575072	2648.321	4615.321
2029	257.164	87.164	5907896	2675.325	4847.512

4.2 Fresh food logistics supply chain distribution optimization results

Selected A city, B city as an example of fruit and vegetable agricultural products supply chain logistics problems. From the distribution of coordinates of A city and B city, it can be seen that the residents of the main residential city uniformly distributed in the two cities near the border line, so choose 4 supply bases (d1-d4) and 26 receiving points (0-25).

First of all, the single city logistics optimization to verify the effectiveness of the algorithm, to A city, for example, take the coordinate number d1, d2 for the supply base coordinates, take 0-12 for the receiving point coordinates, algorithm path optimization convergence curve shown in Figure 5, set the number of iterations for 120 times, the iteration converges to a stable value, that is, the target optimization of the distance cost. The algorithm path optimization is shown in Figure 6, which indicates the result of fresh food logistics supply chain timeliness optimization. Considering the long and narrow topography of city A, the east-west span is too large, the transportation time is too long, and the overall transportation in the city is difficult to be carried out by a supply base across the receiving points in the northwest and southeast, so two independent transportation networks are formed in the north-west and south-east. Algorithm running output to get the optimal path allocation scheme shown in Table 4, while combined with Figure 6 algorithm path optimization results in five optimized paths, and marked with each path detailed constraint parameters. According to the time window set receiving point service time (loading and unloading, etc.), the proposed load (tons), the path of the vehicle limit load is greater than or equal to the sum of the demand for each receiving point, in the optimal path under the premise of the proposed vehicle load can be similarly achieve the optimization purpose. In the actual logistics cost processing, all the results obtained will be converted into actual parameters, for example, the time will be converted into the 24h system, the distance of each path will be calculated separately, and it will be added up and processed with the relevant data such as transportation cost to arrive at the minimum logistics cost.

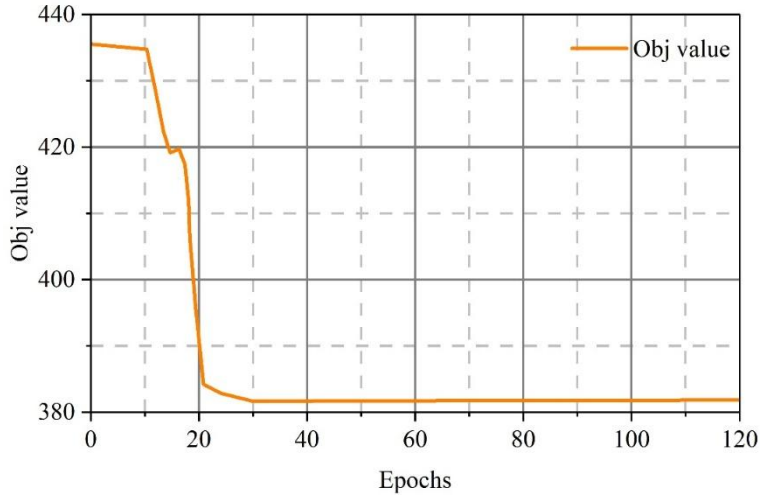

Figure 5: Algorithm path optimization convergence curve

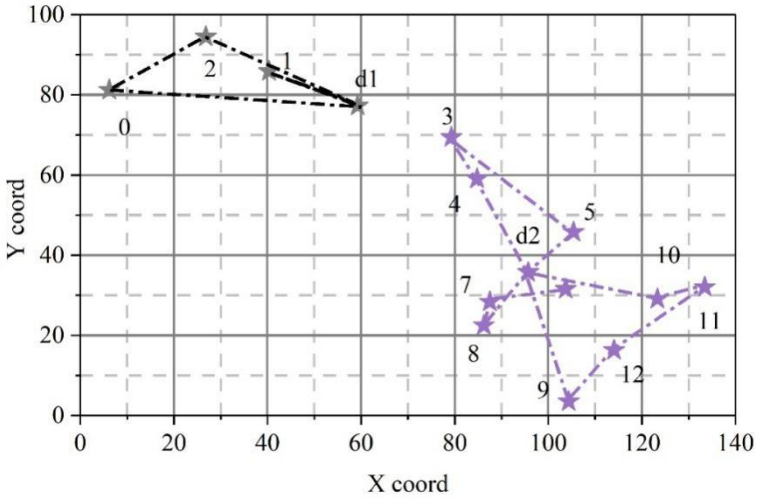

Figure 6: Algorithm path optimization

Table 4: Optimal path allocation scheme

N	Path	Path distance (km)	Transit time (h)	Service time (h)	Recommended deadweight (t)	Distance cost (yuan)
V1	d2-10-11-12-9-d2	1085.5	21.75	7.1	9.2	3900.41
V2	d2-8-7-6-d2	456.1	9.11	5.1	4.2	
V3	d2-4-3-5-d2	808.2	16.17	8.1	8.9	
V4	d1-0-2-d1	1125.5	22.55	4.7	3.2	
V5	d1-1-d1	422.5	8.45	2.9	1.2	

Figure 7 shows the convergence curve of the algorithm path optimization for city A and city B, which indicates that the transportation distance is gradually optimal after iteration; Figure 8 shows the algorithm path optimization for city A and city B, which indicates that 11 paths are obtained after the algorithm optimization. In order to improve the transportation efficiency, each receiving point can only be passed once, and all points should be passed.

The output of the algorithm run yields the optimal path allocation scheme for City A and City B as shown in Table 5, where the suggested load is the sum of the demand of each vehicle at each receiving point in each path, which is used to suggest the approximate amount of cargo required by the vehicle for each shipment. In order for all experimental points to be passed through, there may be a situation where a vehicle only transports one receiving point, for example, vehicles with vehicle numbers V3, V8, and V10 in the optimal path allocation scheme for cities A and B. In order to increase vehicle utilization as well as to reduce the distance cost, there exists cross-city transportation between the two cities bordering on each other. This experiment uses a total of 11 transportation vehicles to get the receiving point and the distance of each path that each vehicle passes through, and the distance cost of the optimal path between city A and city B is 8349.75 yuan.

This experiment adds a penalty time window restriction, which is used to exclude a series of transportation untimely problems in the global optimization process, and the penalty is calculated for overtime within the constraints. The above are the main factors constraining the cost of logistics and transportation, in which various factors interact with each other and need to be iteratively simulated to find the best transportation solution to minimize the total transportation cost. Due to the limitation of cargo capacity, some vehicles may have roughly similar paths, although the paths can be roughly matched, but still need to arrange two transportation vehicles. At the same time, if we consider the loss function, in order to reduce

the loss of agricultural products due to transportation, storage environment, loading and unloading process, the vehicle load must be greater than the recommended load and less than the vehicle's limit load, the specific measures can be to increase in the weight of refrigerated preservation of the use of objects, and so on.

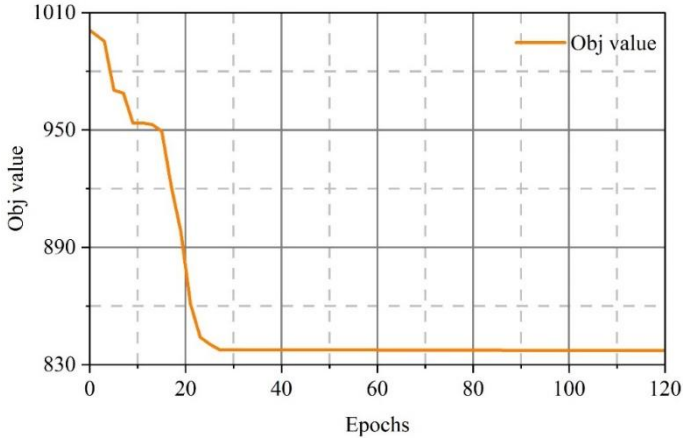

Figure 7: A city and B city path optimization convergence curve

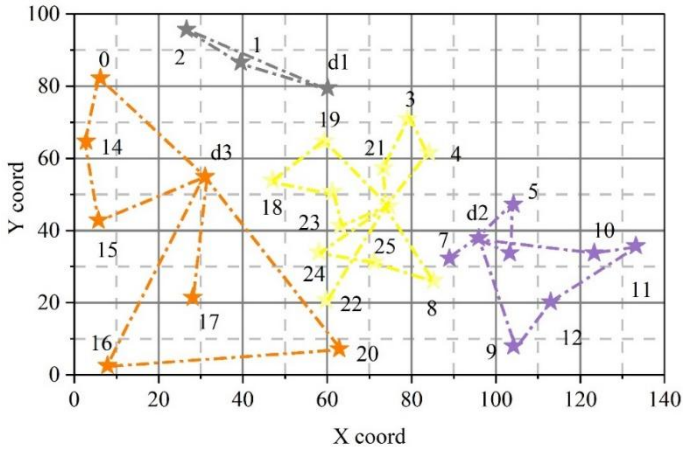

Figure 8: A city and B city algorithm path optimization

Table 5: A city and B city optimal path allocation scheme

N	Path	Path distance (km)	Transit time (h)	Service time (h)	Recommended deadweight (t)	Distance cost (yuan)
V1	d2-10-11-12-9-d2	1085.5	21.75	7.1	9.2	8349.75
V2	d2-6-5-d2	362.5	7.22	5.3	4.2	
V3	d2-7-d2	212.4	4.26	1.1	0.7	
V4	d4-8-25-24-d4	745.4	14.92	6.3	4.8	
V5	d4-23-13-18-19-d4	738.1	14.78	8.7	8.4	
V6	d1-1-2-d1	725.4	14.52	4.5	3.2	
V7	d3-0-14-15-d3	1037.2	20.75	5.6	5.2	
V8	d3-17-d3	663.5	13.25	3.2	2.2	
V9	d3-16-20-d3	1662.1	33.21	2.1	6.3	
V10	d4-22-d4	601.3	12.04	2.7	2.1	
V11	d4-4-3-21-d4	516.7	10.35	7.6	7.4	

5 Conclusion

The study focuses on the problem of optimizing the timeliness in cooperative fresh food logistics, and an integrated decision-making model is proposed for solving the problem, which integrates the forecasting of logistics demands with the optimization of logistics paths in fresh food chains.

To improve the performance of the PSO algorithm, three aspects have been considered, including designing the inertia weight parameter, detecting the environment, and introducing the adaptive jumping mechanism for solutions. With these considerations, the optimization of connection weights and threshold values of the BP neural network can be better realized with the IPSO-BP method. The improved IPSO-BP model is used for the forecasting of the logistics demand for fresh agricultural products in the city. Experiments show that compared with the traditional BP and PSO-BP models, the improved IPSO-BP model demonstrates faster convergence and higher prediction accuracy. The MAPE is 0.15%, which shows that the proposed method is quite applicable to the forecasting of logistics demands that involve nonlinearity.

Further research on the issue is the cooperative optimization of fresh agricultural products in logistics within areas of multiple mountains. The use of storage environment costs, which can ensure the preservation of the quality of the goods during transportation, and combining the simulation annealing algorithm with the ant colony algorithm can improve the global searching capacity in the optimization process. As such, the model proposed can solve path-planning problems under time window constraints, load capacity constraints, and mountainous distribution conditions. Based on time window constraints, load capacity constraints, and mountainous distribution conditions, the cooperative optimization of logistics routes cost and timeliness is realized.

The model presented above shows stable convergence and presents an acceptable route allocation strategy, thus facilitating coordination of multiple vehicles' scheduling, improving the efficiency of logistics operations for fresh produce and providing an appropriate approach to dynamically optimize their delivery routes.

Funding

This work was supported by Research and Development of Key Technologies and Regional Demonstration Application of Intelligent Collaboration in Fresh Food Supply Chain under Instant Consumption Scenario; Research and Application of Data-Driven Digital and Intelligent Logistics Supply Chain Platform (42000025205T00000014402).

About the Author

Xingmin Qi, female, was born in April 1981 in Xiangyang, Hubei Province, P.R. China. She is an Associate Research Fellow at Hubei Institute of Logistics Technology. Her main research direction is logistics information technology research.

Mingcheng Wang, male, was born in October 1978 in Xiangyang, Hubei Province, P.R. China. He holds a Master of Laws degree and serves as a lecturer at the School of Marxism, Nanning University of Technology, P.R. China. His main research direction is Marxist theory.

Xiaowei Xiang, female, was born in September 1989 in Xiangyang, Hubei Province, P.R. China. She serves as an Assistant Research Fellow at Hubei Institute of Logistics Technology, P.R. China. Her main research direction is logistics technology research.

References

[1] Iordăchescu, G., Ploscutanu, G., Pricop, E. M., Baston, O., & Barna, O. (2019). Postharvest losses in transportation and storage for fresh fruits and vegetables sector. Journal of International Scientific Publications, 7, 244-251.

[2] Negi, S., & Trivedi, S. (2021). Factors impacting the quality of fresh produce in transportation and their mitigation strategies: empirical evidence from a developing economy. Journal of Agribusiness in Developing and Emerging Economies, 11(2), 121-139.

[3] Cherono, K., & Workneh, T. S. (2018). A review of the role of transportation on the quality changes of fresh tomatoes and their management in South Africa and other emerging markets. International Food Research Journal, 25(6), 2211-2228.

[4] Ali, A., Xia, C., Ouattara, N. B., Mahmood, I., & Faisal, M. (2021). Economic and environmental consequences' of postharvest loss across food supply Chain in the developing countries. Journal of cleaner production, 323, 129146.

[5] Yang, M., Qu, S., Ji, Y., & Abdoulrahaman, D. (2024). Vulnerability of fresh agricultural products supply chain: Assessment, interrelationship analysis and control strategies. Socio-Economic Planning Sciences, 94, 101928.

[6] Mardenli, A., Sackmann, D., Fiedler, A., Rhein, S., & Alghababsheh, M. (2025). Determinants of information asymmetry in agri-food supply chains. The International Journal of Logistics Management, 36(1), 259-289.

[7] Gao, J., Cui, Z., Li, H., & Jia, R. (2023). Optimization and coordination of the fresh agricultural product supply chain considering the freshness-keeping effort and information sharing. Mathematics, 11(8), 1922.

[8] Chen, Z., Dan, B., Ma, S., & Tian, Y. (2024). Demand information sharing of fresh produce supply chain considering competing suppliers' freshness-keeping effort. International Transactions in Operational Research, 31(2), 1206-1231.

[9] López-Gálvez, F., Gómez, P. A., Artés, F., Artés-Hernández, F., & Aguayo, E. (2021). Interactions between microbial food safety and environmental sustainability in the fresh produce supply chain. Foods, 10(7), 1655.

[10] Aguiar, M. L., Gaspar, P. D., Silva, P. D., Domingues, L. C., & Silva, D. M. (2022). Real-time temperature and humidity measurements during the short-range distribution of perishable food products as a tool for supply-chain energy improvements. Processes, 10(11), 2286.

[11] Malik, A., Li, M., Lenzen, M., Fry, J., Liyanapathirana, N., Beyer, K., ... & Prokopenko, M. (2022). Impacts of climate change and extreme weather on food supply chains cascade across sectors and regions in Australia. Nature Food, 3(8), 631-643.

[12] Sanad Alsbu, R. A., Yarlagadda, P., & Karim, A. (2023). Investigation of the factors that contribute to fresh fruit and vegetable losses in the Australian fresh food supply chain. Processes, 11(4), 1154.

[13] Zhou, Y., Yin, M., Liu, Q., Qian, X., Jin, D., & Lang, X. (2025). Optimizing winner determination for sustainability and timeliness in fresh agricultural product logistics service procurement auctions: insights from a fourth-party logistics perspective. Frontiers in Sustainable Food Systems, 9, 1585053.

[14] Shan, Z., & Yao, J. (2024). Resource Scheduling Optimization of Fresh Food Delivery Porters Considering Ambient Temperature Variations. Sustainability, 16(9), 3624.

[15] Zhao, Z., Li, X., & Zhou, X. (2020). Optimization of transportation routing problem for fresh food in time-varying road network: Considering both food safety reliability and temperature control. PloS one, 15(7), e0235950.

[16] Xie, Y. (2025). A Hybrid Genetic-Neural Optimization Algorithm for Cold Chain Logistics Based on Multivariate Data Mining. Journal of Advanced Manufacturing Systems, 1-27.

[17] Bisenovna, K. A., Ashatuly, S. A., Beibutovna, L. Z., Yesilbayuly, K. S., Zagievna, A. A., Galymbekovna, M. Z., & Oralkhanuly, O. B. (2024). Improving the efficiency of food supplies for a trading company based on an artificial neural network. International Journal of Electrical and Computer Engineering, 14(4), 4407-4417.

[18] Chen, Y., Wu, Q., & Shao, L. (2020). Urban cold-chain logistics demand predicting model based on improved neural network model. International Journal of Metrology and Quality Engineering, 11, 5.

[19] Li, T., Wang, S., Nong, T., Liu, B., Hu, F., Chen, Y., & Han, Y. (2025). Bayesian Optimization of LSTM-Driven Cold Chain Warehouse Demand Forecasting Application and Optimization. Processes, 13(10), 3085.

[20] Kumar, G. S., Siddartha, J., Nayan, M. V. S., & Bhadru, L. (2025). REAL TIME SHELF LIFE PREDICTION OF FRESH PRODUCE USING CNN BASED TEMPERATURE ANALYTICS. International Journal of Data Science and IoT Management System, 4(3), 134-142.

[21] Chołodowicz, E., & Orłowski, P. (2022). Control of perishable inventory system with uncertain perishability process using neural networks and robust multicriteria optimization. Bulletin of the Polish Academy of Sciences Technical Sciences, e141182-e141182.

[22] Teng, S. (2021). Route planning method for cross-border e-commerce logistics of agricultural products based on recurrent neural network. Soft computing, 25(18), 12107-12116.

[23] Zou, Y., Wu, J., Wang, X., Morales, K., Liu, G., & Manzardo, A. (2023). An improved artificial neural network using multi-source data to estimate food temperature during multi-temperature delivery. Journal of Food Engineering, 351, 111518.

[24] Yang, J., & Wang, S. (2026). Intelligent Heat and Humidity Control System for Agricultural Product Warehousing and Logistics Using High-Throughput Humidification and Fuzzy Q-Learning Optimization. Journal of Circuits, Systems and Computers.